Chapter 5

A genetic interaction screen reveals a new signalling pathway

5.1 Introduction

The clear increase in scale that parallel phenotyping by barcode sequencing provided offers new opportunities for reverse genetic screening that were previously unachievable for malaria parasites. One of these is the study of genetic interactions at scale. The last aim of this project was therefore to demonstrate that such studies are now possible in *P. berghei* parasites.

Genetic interactions result from the interplay between genes that have a function either within the same pathway or between interconnected pathways. In model organisms, systematic screens for genetic interactions have provided deep insights into biological pathways [100,102].

Since I have demonstrated in Chapter 3 that in *P. berghei* the likelihood of manipulating two loci simultaneously is negligible, this kind of study requires sequential manipulations of the genome. This has become more feasible in *P. berghei* parasites since the development of a positive-negative recyclable selection cassette [54]. As this cassette is part of all *Plasmo*GEM vectors, I generated a panel of marker free mutants that were used as background lines to repeat the ePK deletion screen described in Chapter 4. This approach allowed me to look at the fitness of dozens of double mutants in the same experiment and revealed a case of epistasic genetic interaction in the *P. berghei* kinome.

5.2 Results

5.2.1 Choice of the genetic backgrounds

CDPKs are protein kinases that are found in apicomplexan parasites and plants. This makes them very attractive targets for antimalarial drug development [139,170,188]. *P. berghei* parasites have six CDPKs. This family of protein kinases has been shown to control important signalling processes in these parasites such as motility, development and egress [136,138,144,189]. Due to their pivotal role in so many aspects of the parasite's life cycle it is surprising that four out of six are dispensable for blood stage development. In fact, *cdpk1* and *cdpk4*, were even reported to be expressed at the protein level in blood stages [34,62]. We therefore hypothesised that this seeming genetic redundancy among the CDPKs was, in fact, the result of genetic buffering, i.e. the existence of compensatory effects amongst

them. For this reason the targetable CDPKs were chosen as the genetic backgrounds against which genetic interactions were searched for. Additionally, two other genetic backgrounds were selected: a resistant allele of the *pkg* gene (*pkg*^{T619Q})[9], and a double KO mutant for the MAP kinases.

The *pkg* gene encodes a protein kinase that is activated by cGMP. The binding of this secondary messenger promotes the phosphorylation of a number of biologically important targets in higher eukaryotes, being implicated in the regulation of smooth muscle relaxation, platelet function, sperm metabolism, cell division, and nucleic acid synthesis [190].

In *Plasmodium*, *pkg* is an essential gene for blood stage development. Therefore, its function has been studied through a chemical genetics approach. According to this strategy, a mutation of the amino-acid that controls the access of small molecules to the ATP-binding pocket, the so-called gatekeeper residue, generates a mutant line that is selectively resistant to an inhibitory compound without compromising the functionality of the enzyme [191]. Parasite growth is strongly impaired in the presence of Compound 1 (a trisubstituted pyrrole 4-[2-(4-fluorophenyl)-5-(1-methylpiperidine-4-yl)-1H-pyrrol-3-yl] pyridine (C1)), a reversible but potent and selective inhibitor of PKG. A single point mutation in the *pkg* gene to replace the small threonine residue with a bulky glutamine one (T619Q in *P. berghei* and T618Q in *P. falciparum*) is sufficient to render parasites resistant to this chemical without affecting parasite growth [192,193].

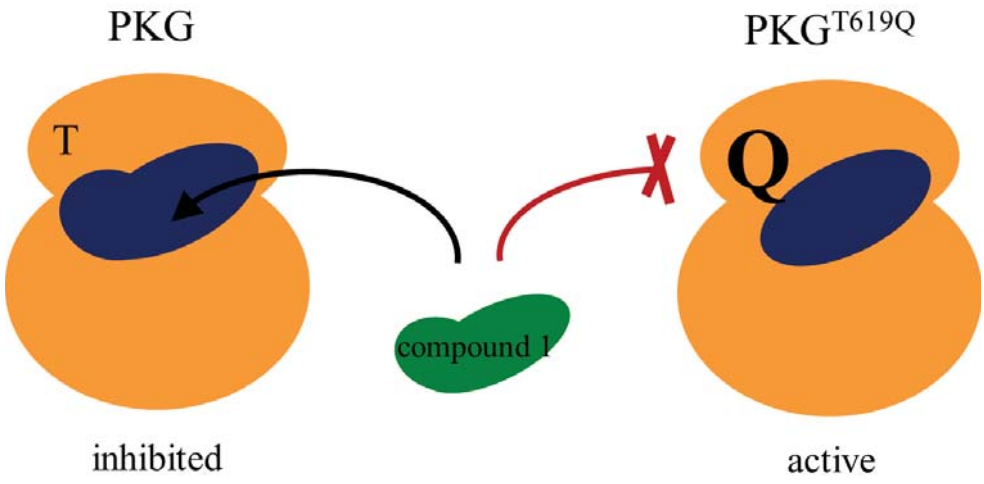

Fig. 5.1| The mutation of the gatekeeper amino-acid renders PKG resistant to Compound 1.
PKG has a small threonine (T619 in *P. berghei*) gatekeeper residue that when mutated into a glutamine (Q) residue, prevents the binding of the compound. This compound selectively inhibits the parasite PKG and not the host since the metazoan PKG has a large gatekeeper.

[9] This line was kindly provided by Mathieu Brochet [154].

Comparative analyses of the effect of this compound in WT and resistant lines revealed that PKG plays crucial roles throughout development. For instance, transient inhibition of PKG impairs schizogony [192] and gametogenesis [194] of *P. falciparum* parasites. Furthermore, it has also been shown that in *P. berghei* gametocytes, stimulation with XA is followed by mobilisation of intracellular calcium through the activation of PKG and possibly PI-PLC [154]. The observation that PKG activation is required for regulation of cytosolic levels of calcium, which in turn regulate CDPKs, led us to include the resistant *pkg*^{T619Q} allele in the screen.

The MAP cascade is highly conserved in eukaryotes. MAP kinases are responsible for regulation of important cellular processes, like mitosis, differentiation, and cell survival. They are activated through extracellular stimuli, such as mitogens, osmotic stress or pro-inflammatory cytokines [127]. However, very little is known about its role in *Plasmodium* parasites as they lack the canonical upstream regulators and downstream effectors of these kinases [119]. The overexpression of Pb*map2* transcripts in mutants lacking Pb*map1* (Volker Heussler, personal communication) suggested the existence of a compensatory effect if not an interaction between these two genes. Given the relevance of these kinases in other organisms and our gap in knowledge about this pathway in *Plasmodium* parasites, I attempted to generate a double KO (dKO) mutant for both *map* kinases (see section 5.2.2.1). As this mutant was unexpectedly viable, indicating that perhaps there is a third kinase with overlapping functions, this double mutant was used as a genetic background in the genetic interaction screen.

5.2.2 Generation of selection marker free backgrounds

A total of six different genetic backgrounds were produced to look at genetic interactions between ePKs. Firstly, single KO mutants for each of the chosen genes (*cdpk1*, *cdpk3*, *cdpk4*, *cdpk6*, *pkg*^{T619Q} and *map1*) were generated. These lines were then cloned and their selection cassette was excised [54] with negative selection. A final dilution cloning step ensured that these marker free lines were clonal and suitable to be used as genetic backgrounds for the genetic interaction screen. This workflow was repeated twice to generate a double KO for the *map* kinase genes. Figure 5.1 A-D shows Southern blot and PCR genotyping results for each of the *cdpk* mutants. For each of the Southern blots I used two different probes: one that targeted a sequence present in both the WT and the mutant and another probe that only targeted the gene sequence. The former should display the difference

in the size of the locus after removal of the gene while the latter ensured that very rare cases of gene duplications (e.g. *rio2* KO mutants) would not go unnoticed.

All mutants were successfully obtained, and genotyping was unambiguous.

5.2.2.1 Phenotypic analysis of the *map* double KO revealed a *map2* KO-like phenotype

While the *map1* gene can be disrupted in both *P. berghei* and *P. falciparum* parasites, *map2* is required for the asexual development in *P. falciparum* but not in *P. berghei* [129]. In *P. berghei*, *map1* seems completely dispensable, while *map2* is required for microgametogenesis, specifically genome replication and cytoskeletal rearrangements associated with mitosis and assembly of axonemes [138]. However, despite this crucial role during gamete formation the *Pbmap2* gene can be targeted in blood stages. In fact, both *map* genes could be disrupted simultaneously in *P. berghei* (Fig 5.3 A, B). The phenotype of this double mutant was not noticeably different from the WT in the asexual blood stages (Fig. 5.3C), but it showed a sexual phenotype similar to the *map2* KO alone. Figure 5.3D and E show the highly reduced ookinete conversion rate which was a result of the blockade in microgamete exflagellation, confirming the previous analysis of the *map2* single mutant [138].

As both kinases were successfully disrupted it is possible that there is a third kinase that is up-regulated in the absence of the other two.

Fig. 5.2| Genotyping of CDPK KO genetic backgrounds (next two pages)
The genotype of each of the CDPK mutants was confirmed by Southern blot of restricted gDNA (top panel of each Figure) and PCR (bottom panel). Two different probes were used to hybridise the DNA fragments on the Southern blots. One probe should detect both loci, but show a difference in the size as consequence of gene removal, and another that should only hybridise with the WT gene sequence and therefore not with the mutant DNA. The restriction digest strategy is illustrated next to each blot. For the PCR genotyping eight reactions were performed to distinguish three different gDNAs: the WT, the mutant after the first round of cloning and the cloned mutant after resistance cassette removal. These included one positive control (*rna polymerase II*), two reactions targeting the WT gene (5' and 3' end), three others targeting the modified locus resistance cassette (two detected the presence of the vector and the third detected correct integration), one reaction across the gene that should generate differently sized bands for each of the three gDNAs (this reaction was particularly important to identify excision of the resistance cassette), and one last reaction that detected the parasite's resistance cassette. (A-D) Genotyping of *cdpk1* KO, *cdpk3* KO, *cdpk4* KO, and *cdpk6* KO mutants, respectively.
Note that the white asterisk (*) in the middle panel of the gel picture in Figure B (*cdpk3* KO genotyping) denotes the band with the correct size. In Figure C, the presence of two bands on the left panel of the Southern blot is the result of incomplete digestion by *Hind*III enzyme that is present twice downstream the *cdpk4* gene, depicted on the Southern blot map on the left.

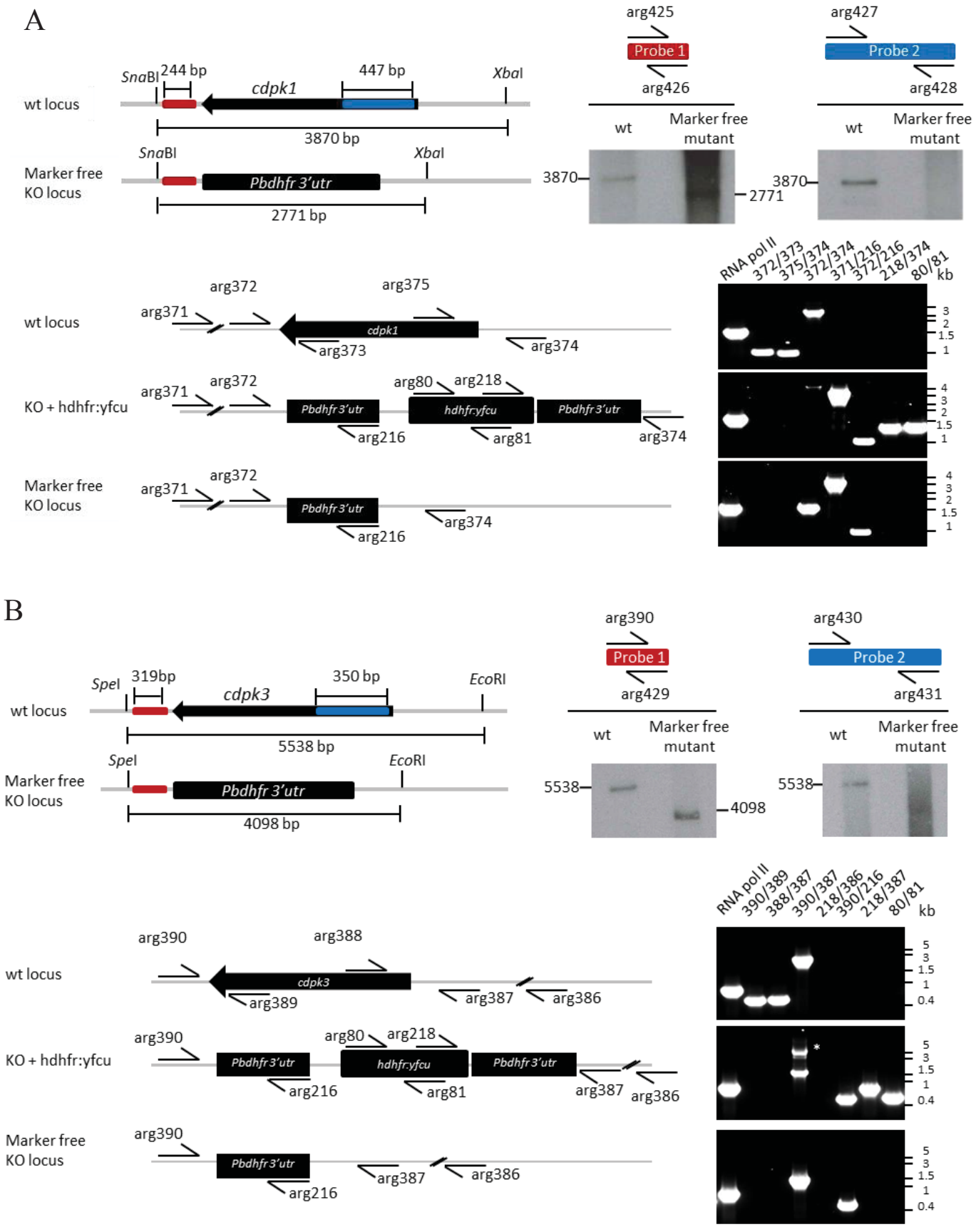
A
wt locus
SnaBI
244 bp
cdpk1
447 bp
XbaI
3870 bp
Marker free
KO locus
Pbdhfr 3'utr
2771 bp
arg425
Probe 1
arg426
arg427
Probe 2
arg428
wt
Marker free
mutant
3870
2771
RNA pol II
372/373
375/374
372/374
371/216
372/216
218/374
80/81
kb
arg371
arg372
arg375
arg373
arg374
KO + hdhfr:yfcu
arg80
arg218
hdhfr:yfcu
arg216
arg81
B
SpeI
319bp
cdpk3
350 bp
EcoRI
5538 bp
4098 bp
arg390
arg388
arg389
arg387
arg386
arg429
arg430
Probe 1
Probe 2
arg431
5538
4098
390/389
388/387
390/387
218/386
390/216
218/387
80/81

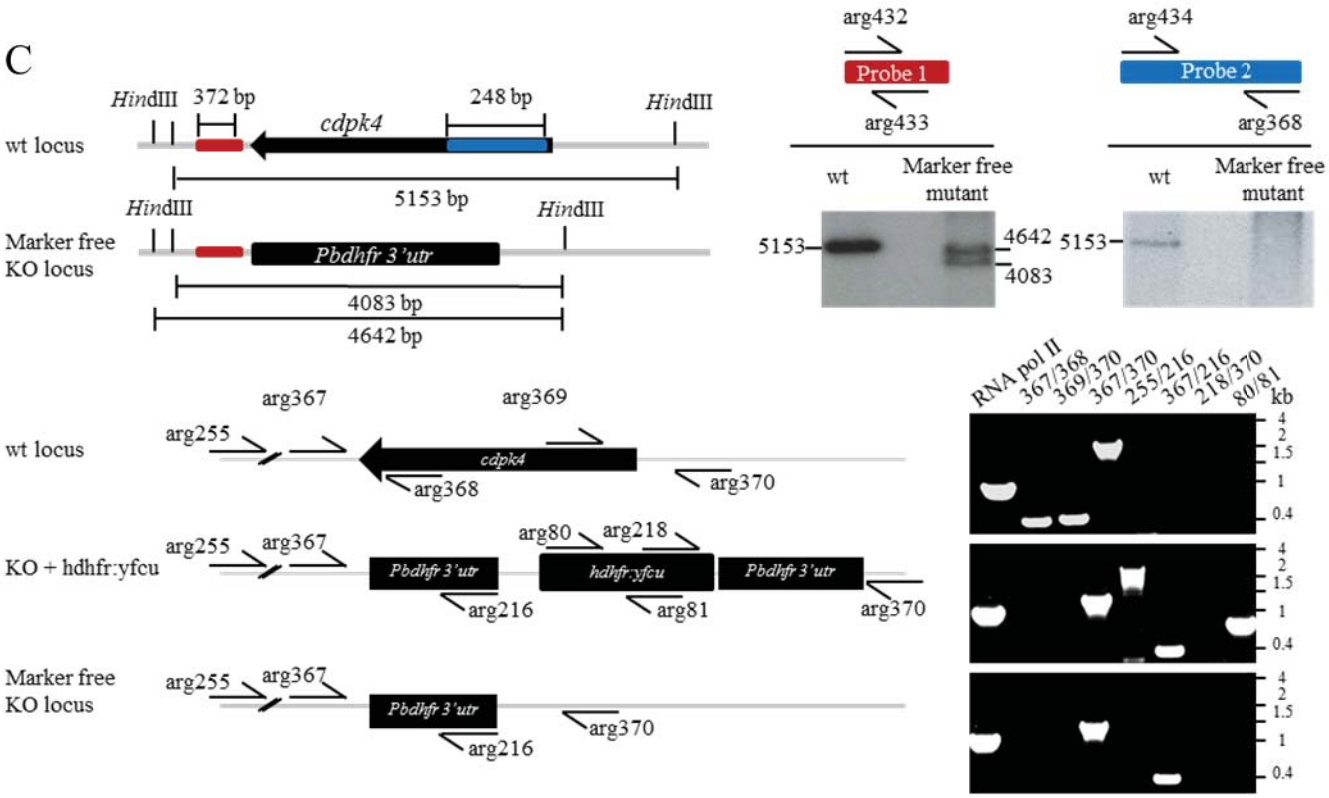
C
HindIII
372 bp
cdpk4
248 bp
HindIII
wt locus
5153 bp
HindIII
HindIII
Marker free
KO locus
Pbdhfr 3'utr
4083 bp
4642 bp
arg432
Probe 1
arg433
arg434
Probe 2
arg368
wt
Marker free
mutant
5153
4642
4083
arg367
arg369
arg255
wt locus
cdpk4
arg368
arg370
arg80
arg218
KO + hdhfr:yfcu
Pbdhfr 3'utr
hdhfr:yfcu
Pbdhfr 3'utr
arg216
arg81
Marker free
KO locus
RNA pol II
367/368
369/370
367/370
255/216
367/216
218/370
80/81
kb
4
2
1.5
1
0.4

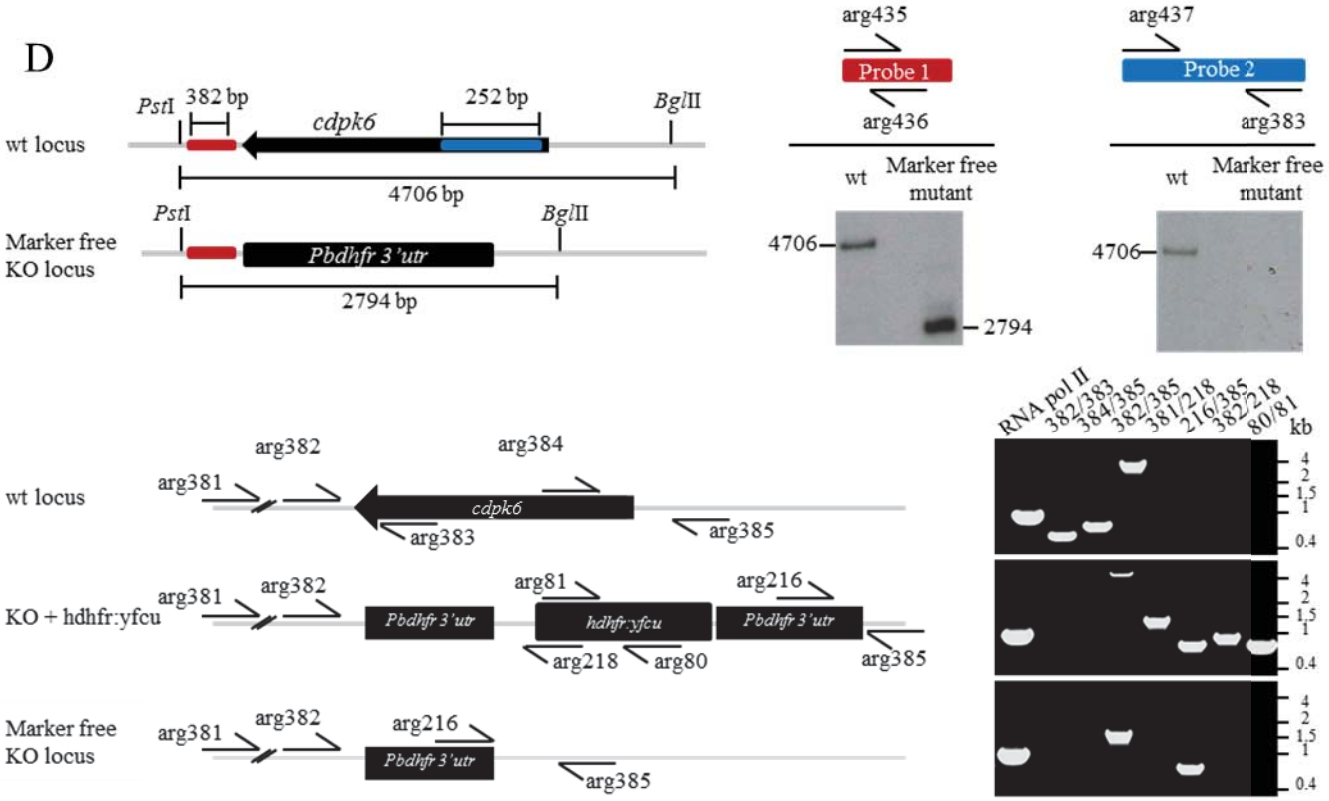
D
PstI
382 bp
cdpk6
252 bp
BglII
wt locus
4706 bp
PstI
BglII
Marker free
KO locus
Pbdhfr 3'utr
2794 bp
arg435
Probe 1
arg436
arg437
Probe 2
arg383
wt
Marker free
mutant
4706
2794
arg382
arg384
arg381
wt locus
cdpk6
arg383
arg385
arg81
arg216
KO + hdhfr:yfcu
Pbdhfr 3'utr
hdhfr:yfcu
Pbdhfr 3'utr
arg218
arg80
Marker free
KO locus
RNA pol II
382/383
384/385
382/385
381/218
216/385
382/218
80/81
kb
4
2
1.5
1
0.4

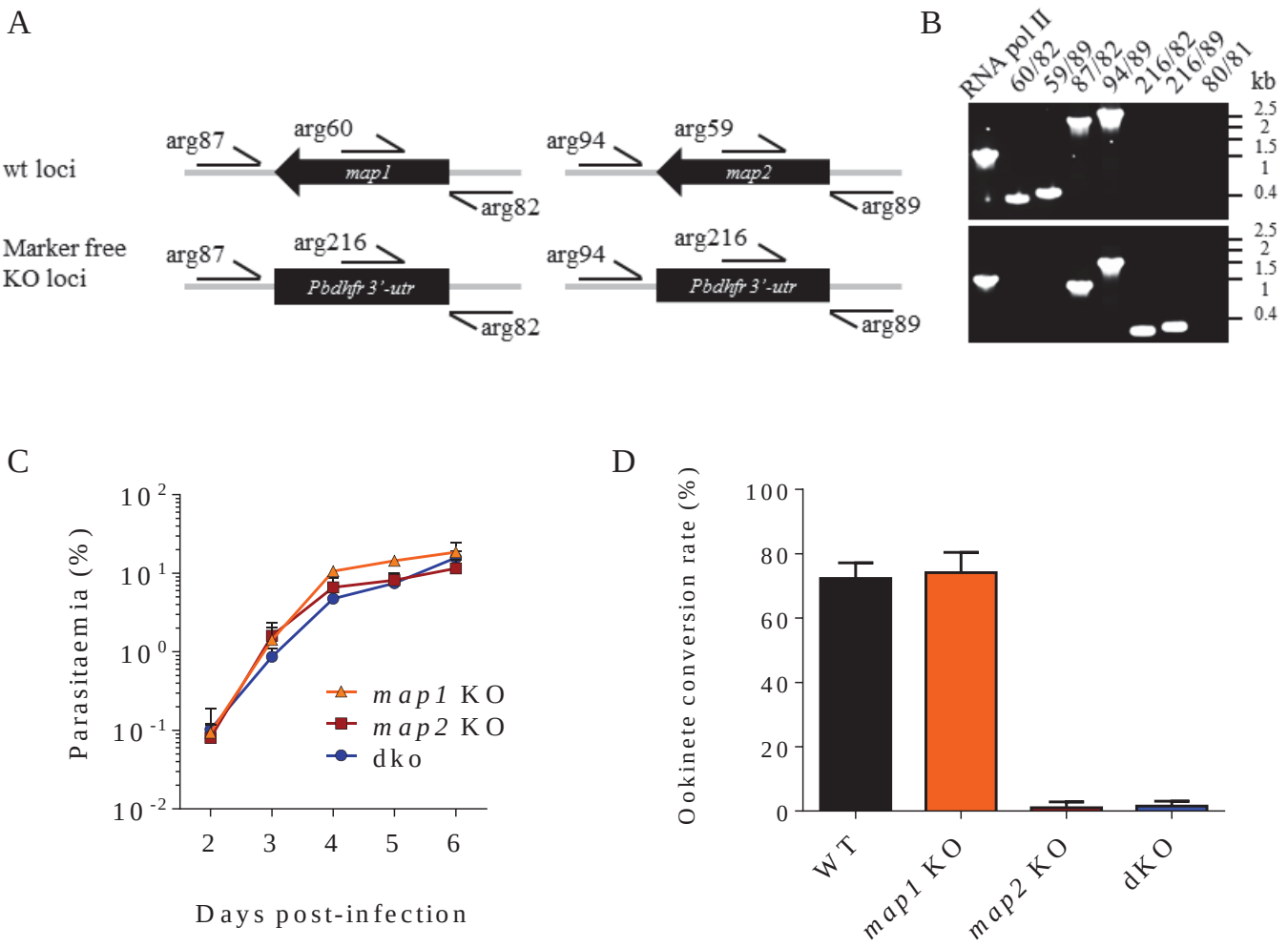

Fig. 5.3| Genotyping and phenotyping of the double KO mutant *map1*$^{-}$/*map2*$^{-}$ (dKO).
(A,B) PCR confirmation of the genotype of the dKO mutant. (A) Illustration of the primer annealing sites. (B) Eight reactions were performed to genotype the final mutant. One positive control (RNA polymerase II), two reactions to detect either *map1* or *map2* genes, two others that spanned each of the gene's ORF to detect excision of the drug cassette, two more reactions to detect the 3' end of each of the modified loci and one last PCR to detect the presence of the complete resistance cassette. (C-D) Phenotyping of the dKO mutant. (C) Comparison of the growth patterns of the cloned single *map* mutants (no detectable fitness cost) to the dKO mutant. (D) Ookinete conversion rate was greatly impaired in the dKO mutant as it was in the single *map2* KO. Three different cultures were sampled twice for each parasite line. (E) Imaging of one of the ookinete cultures used to calculate the conversion rate in (D). Parasites were stained with anti-P28 Cy3-labeled monoclonal antibody and

Hoechst to label the DNA. Most parasites in the double KO culture were non-fertilised female gametes (i.e. round forms) rather than banana-shaped ookinetes as the ones found in the WT culture (top panel). Scale bar = 5μm.

5.2.3 Revealing epistasis in the *P. berghei* kinome

The experiments performed on the WT background (Chapter 4) became an important control for this interaction screen as I used the same vector stocks to generate the DNA pools. Each pool lacked the targeting vector that had been used to generate the corresponding background but no other changes were implemented.

One immediate consequence of using a KO line as the genetic background in an STM experiment is the presence of two barcodes in each mutant parasite, i.e. one from the background and another one from the DNA transfected during the screen. This number is increased to three barcodes in the case of the dKO, where each background carries two barcodes that together should account for $^2/_3$ of the total barcode counts, per time-point.

At the moment of transfection, the genetic background accounts for 100 % of the parasite barcodes. As the new set of barcodes integrates and the drug selection clears the non-transfected parasites, this percentage should decrease to 50 % (or 33.3% in case the where the background has two barcodes).

Indeed, the analysis of the counts for the background barcodes over time showed that they stabilised on ~50 % and ~33% as expected (Fig. 5.4). However this only happened, from day 6 post-transfection onwards, which suggested that it takes approximately four to five days for the drug selection (and the spleen clearance) to clear all the parasites that did not integrate a new vector. Day 4 post-transfection was the time-point with the most excess of background counts relatively to the newly transfected barcode.

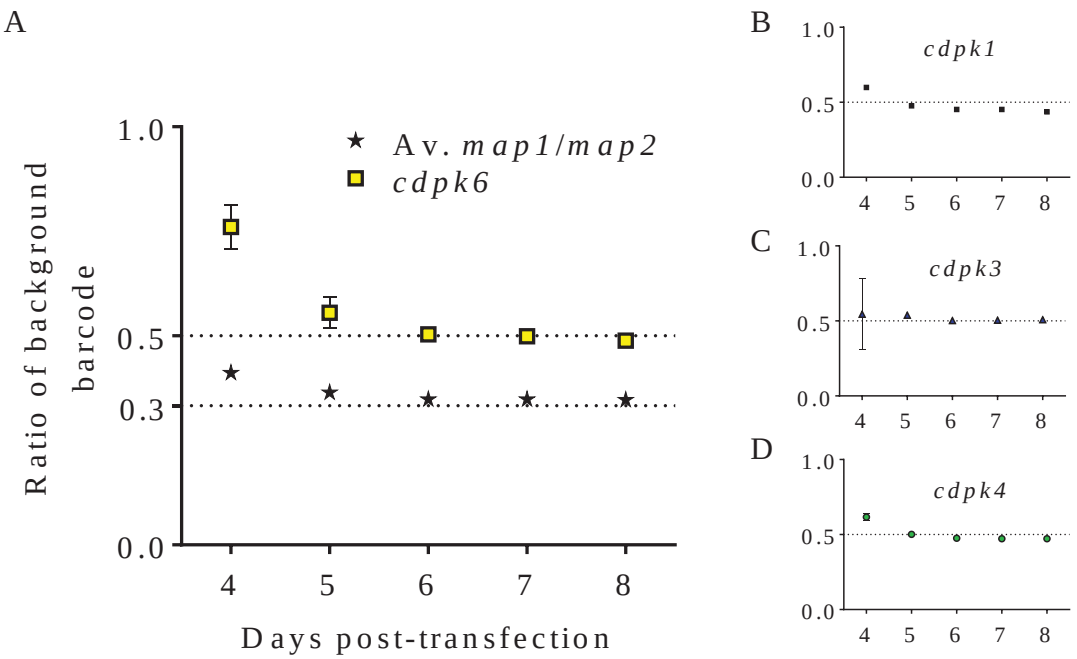

Fig. 5.4| Analysis of the genetic background barcode counts.
The pool of vectors studied in chapter 4 was then re-transfected in each of these background lines without the vector(s) targeting the already deleted loci in each particular case. The proportion of the barcode corresponding to the genetic background for each of the parasite lines was calculated for (A) *cdpk6* KO and dKO; (B) *cdpk1* KO; (C) *cdpk3* KO and (D) *cdpk4* KO. Note that in (A) it is the average of the proportion of barcode counts for *map1* and *map2*.

Six parallel transfections yielded fitness data for 258 double or triple mutants. Using a multiplicative model of epistasis [101], interaction coefficients were determined from the relative fitness phenotypes of the individual mutations and the fitness of the double (or triple) mutants (Fig. 5.5A,B).

Two putative interactions, one positive and one negative were detected and are highlighted in green and red, respectively.

A severe growth defect was detected for a mutant lacking the otherwise redundant *cdpk4* gene on a line expressing the resistant *pkg*^{T619Q}3xHA allele [154] (red circle). This suggested the existence of an important genetic interaction between *cdpk4* and *pkg* and was therefore validated with independently generated mutants, as described in the next section.

The positive interaction was detected for the pair *cdpk3* x PBANKA_146050 and was characterised by an increased fitness of the double mutant compared to the individual mutants (1.0 and 0.9, respectively). This proved to be specific to the pair *cdpk3* x PBANKA_146050.

PBANKA_146050 KO mutants fail to differentiate into ookinetes efficiently. The few that establish a mosquito infection do not produce sporozoites. This gene is *gak* (cyclin G-associated kinase) and its orthologue has been implicated in cell cycle progression due to a role in clathrin-mediated membrane trafficking [195]. *cdpk3*, on the other hand, has been associated with ookinete motility triggered by calcium signaling. Its disruption greatly decreases the ookinete ability to infect the mosquito midgut [136].

The link between these two genes is unknown and due to time constraints I did not pursue this putative interaction further.

All grey circular symbols in Figure 5.5B show data points in which targeting vectors integrated with borderline efficiency and fitness calculations were based on too few read counts to be considered reliable. These were hits that included the genes *srpk* and PBANKA_040940, both of which considered technical fails of the respective vectors for unknown reasons as evidence from others showed that they are targetable [105].

A

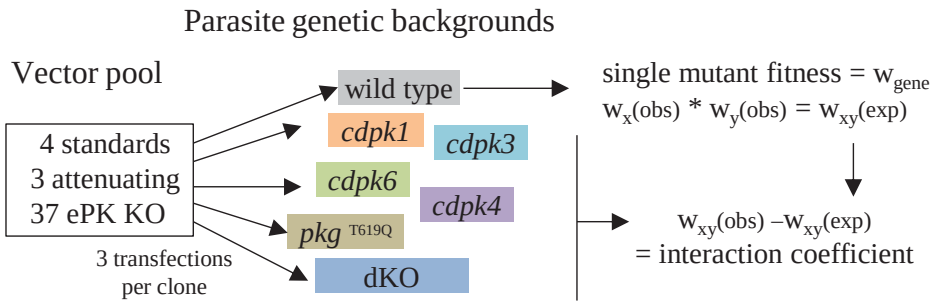
Parasite genetic backgrounds
Vector pool
4 standards
3 attenuating
37 ePK KO
3 transfections per clone
wild type
cdpk1
cdpk3
cdpk6
cdpk4
pkg T619Q
dKO
single mutant fitness = w_{gene}
$w_x(obs) * w_y(obs) = w_{xy}(exp)$
$w_{xy}(obs) - w_{xy}(exp)$
= interaction coefficient

B

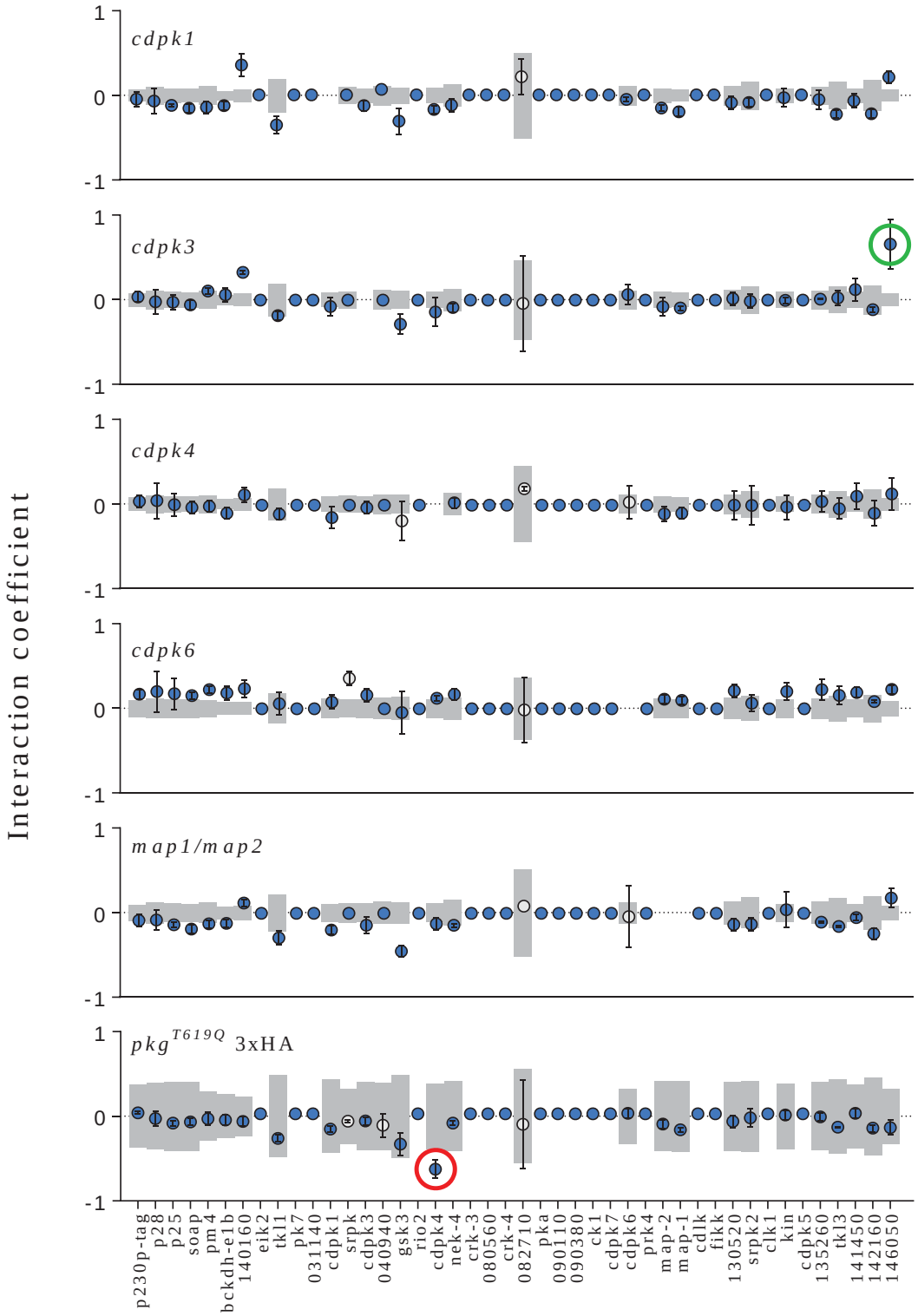
Interaction coefficient
cdpk1
cdpk3
cdpk4
cdpk6
map1/map2
pkg T619Q 3xHA
1
0
-1
p230p-tag
p28
p25
soap
pm4
bckdh-e1b
140160
eik2
tkl1
pk7
031140
cdpk1
srpk
cdpk3
040940
gsk3
rio2
cdpk4
nek-4
crk-3
080560
crk-4
082710
pka
090110
090380
ck1
cdpk7
cdpk6
prk4
map-2
map-1
cdlk
fikk
130520
srpk2
clk1
kin
cdpk5
135260
tkl3
141450
142160
146050

Fig. 5.5| Interaction coefficients for 258 double and triple mutants (next page).
(A) Schematic illustration of the interaction study. The interaction coefficient between two genes is defined as the difference between the observed fitness (W_{obs}) of a double mutant and its expected fitness (W_{exp}). The latter assumes that there is no interaction between the genes and that the fitness of the double mutant is the result of a cumulative effect of both mutations. (B) Genetic interaction coefficients on day 7 post-transfection (blue symbols). The "no interaction" area has been delimited by grey bars and reflects the combined uncertainty (two standard deviations) of the combined fitness measurements. In some cases, low barcode counts (< 0.25 % of the total) led to potentially inaccurate coefficient calculations. These are therefore shaded grey.
Green and red circles highlight putative positive and negative interactions, respectively. Mutants not viable were included in the graph as having a coefficient of zero. The absence of the grey bar was the result of no fitness values (i.e. likely essential gene) for the corresponding single mutant. Note that because the *pkg*^{T619Q} mutant does not carry a barcode, its fitness was calculated from parasitaemia growth curves. This slightly less accurate method of calculating the single mutant fitness is the reason for the uncertainty grey boxes being larger than in the other mutants.
Error bars show standard deviations of the mean of W(obs) (n=3).

5.2.4 Validation of *cdpk4*-*pkg* interaction

The work presented in this section was mostly performed in collaboration with Mathieu Brochet and is shown here due to its relevance for the project.

The analysis of the interaction coefficients suggested the existence of an interaction between *pkg* and *cdpk4*. Statistical analysis of the fitness of the double mutant indicated that it was significantly different from the normal growth references, throughout infection (Fig. 5.6A).

In order to validate this putative interaction, a double mutant was generated independently, by disruption of the *cdpk4* gene in the same strain used for the screen (*pkg*^{T619Q}). Careful examination of the growth pattern of the double mutant in comparison with the WT and the single mutant *cdpk4* KO was also indicative of a strong fitness cost caused by the double mutation (Fig. 5.6B).

Western blot analysis of schizont extracts from a parasite strain expressing *cdpk4*-3xHA but defective for production of gametocytes [196] showed that *cdpk4* is not only expressed in gametocytes as previously shown [138], but also in asexual stages as is *pkg* (Fig 5.6C), in agreement with proteomic analyses previously published [34].

Next, complementation of the double mutant was performed by either re-introducing the *cdpk4* gene or by repairing the gatekeeper mutation. This complementation strategy generated the following genotypes: *pkg*^{T619Q}3xHA/*cdpk4*-3xHA and *pkg*-3xHA/*cdpk4* KO, respectively and their growth patterns are depicted in Figure 5.6D. Although successful, neither of the strategies restored growth of the complemented mutants to WT levels. These results suggested

that the epitope tag and / or the generic 3'UTR used in both complementation vectors imposed a moderate fitness cost and generated hypomorphic alleles.[10] A complementation strategy with vectors that do not carry a 3xHA epitope tag has been devised and work is ongoing.

Altogether, these findings support the existence of a genetic interaction between *pkg* and *cdpk4*.

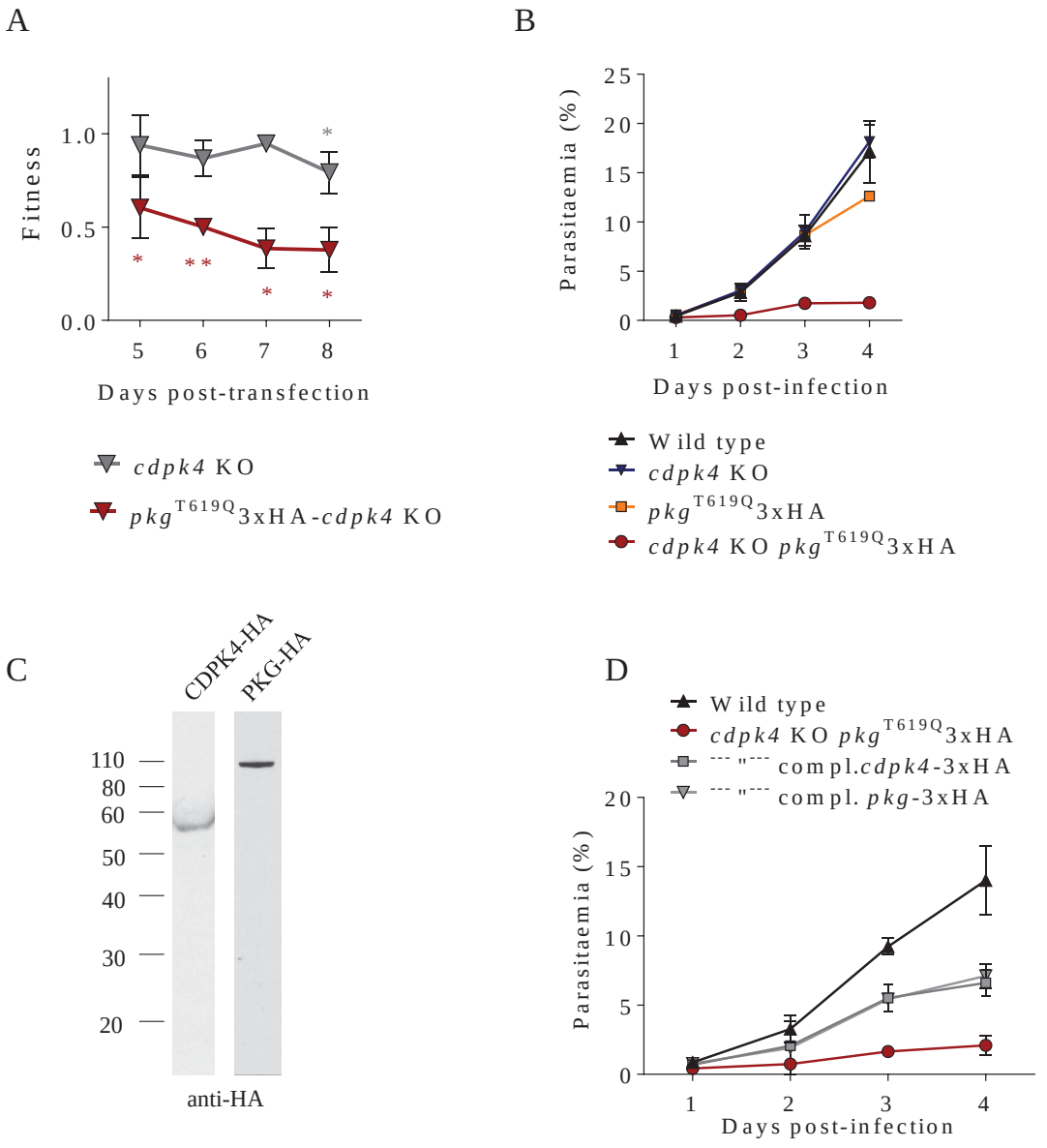

Fig. 5.6| The genetic interaction between *cdpk4* and *pkg* was also detected in independently generated mutants. (A) Bar-seq data showing a fitness comparison between the highly attenuated double mutant pkg^{T619Q}3xHA and *cdpk4* KO. Error bars show standard deviations from the mean (n=3). *Different from the WT reference mutants (included in all experiments) as determined by a two sided T-test corrected for multiple testing; *p < 0.05, **p < 0.01. (B) Growth curves of independently generated mutants over four days of infection determined from

[10] A hypomorphic allele is an allele with reduced levels of gene activity.

Giemsa stained smears. (C) Western blot performed on total protein extracts from *cdpk4*-3xHA and *pkg*-3xHA schizonts showed that both proteins are expressed during the asexual stages. The membrane was probed with an anti-HA antibody. The expected sizes were ~60 KDa and ~100 KDa, respectively. (D) Growth pattern of the complemented mutant lines and respective parental line. Each mutation, *cdpk4* KO and pkg^{T619Q}, was complemented independently. The grey squares represent the mutant where the *cdpk4* locus was restored and the inverted grey triangles show the mutant where the *pkg* point mutation was corrected.

5.3 Discussion

Redundancy between pathways ensures robustness of biological processes. This is the reason why in most organisms a remarkable proportion of genes can be disrupted without compromising viability. For instance, only 20 % of yeast genes are required for haploid development in optimal culturing conditions [100]. This network buffering complicates the analysis of traditional reverse genetics studies.

Systematic analyses in *S. cerevisiae* have shed light on important properties of genetic networks and their components. These have shown that synthetic interactions are highly biased toward genes that have related functions [102] and have connected genes that despite performing related functions lacked a direct functional relationship. For instance, the *rfc5* gene which encodes a subunit of the replication factor C and is required for the checkpoint that responds to replication block and DNA damage [197] was shown to interact with *nse1* and *smc6*, both members of a complex responsible for structural maintenance of chromosomes [198].

The screening approach presented here shows for the first time that synthetic interactions can be revealed through a genetic screen in *Plasmodium*. In this chapter I have shown that deletion screening by barcode counting on different genetic backgrounds enables growth phenotyping of dozens of double or triple mutants in the same mouse, in the timeframe of a normal transfection.

The screen revealed a negative interaction between *pkg* and *cdpk4*. The double mutant had a marked growth disadvantage that was validated by independent generation of the mutant. A function for *cdpk4* in blood stages was surprising as CDPK4 has been shown to be a major sexual stage regulator [138,189]. PKG, on the other hand has been shown to control the intracellular levels of calcium by regulating the biosynthesis of phosphoinositides [154]. A direct genetic interaction between *pkg* and *cdpk4* had never been documented.

Calcium plays a critical role in merozoite egress. During the last hour of *P. falciparum* erythrocytic cycle, merozoite egress is initiated by the release of calcium from the endoplasmic reticulum (ER) stores in a PKG dependent fashion [154]. This event promotes: (1) activation of CDPK5 and CDPK4, (2) induction of calcium-dependent vacuole swelling (3) destabilization of the RBC cytoskeleton [199,200]. Activation of PKG also triggers the secretion of organelles called micronemes and the discharge of the protease PfSUB1 into the parasitophorous vacuole that is responsible for modifying merozoites surface proteins as part of the egress process [201].

Our knowledge of the exact role of CDPKs in egress is still very rudimentary, but a link between *pkg* and *cdpk5* and their function in blood stage merozoites egress has been reported in *P. falciparum* [201]. Dvorin and colleagues showed that the depletion of CDPK5 prevents mature schizonts from egressing despite normal maturation of egress factors. Physical disruption of these schizonts released infectious merozoites [144]. In this study the depletion of CDPK5 was achieved with a destabilisation domain (DD) strategy. A transcriptome analysis of these arrested mutants was subsequently performed 48 hours after removal of shield. As this dataset is publicly available, I looked at the effect of CDPK5 depletion on *cdpk4* and found that the *cdpk4* transcript was ranked in the top 1 % of down-regulated genes. Unfortunately, the lack of replicates and technical details prevented statistical analysis of this dataset. Nevertheless, this is an indication that CDPK5 and CDPK4 might be part of the same pathway. In light of these data it is tempting to propose the following hypothetical model of parasite egress (Fig. 5.7):

(A) In WT parasites, activation of a fully functional PKG triggers microneme secretion and calcium release. This stimulus activates CDPK5 and CDPK4 that cooperatively promote merozoites egress upon microneme and exoneme secretion.

(B) A less efficient egress could be the cause for the reduced growth rate of the double mutant parasites. It has recently been shown that PKG^{T619Q} mutants, although viable throughout the life cycle [154], are less efficient at triggering calcium release (Mathieu Brochet, personal communication). This decreased level of intracellular calcium which does not seem to affect activation of the egress pathways in single mutants becomes critical in the absence of CDPK4, perhaps because CDPK5 on its own is unable to efficiently trigger merozoites release.

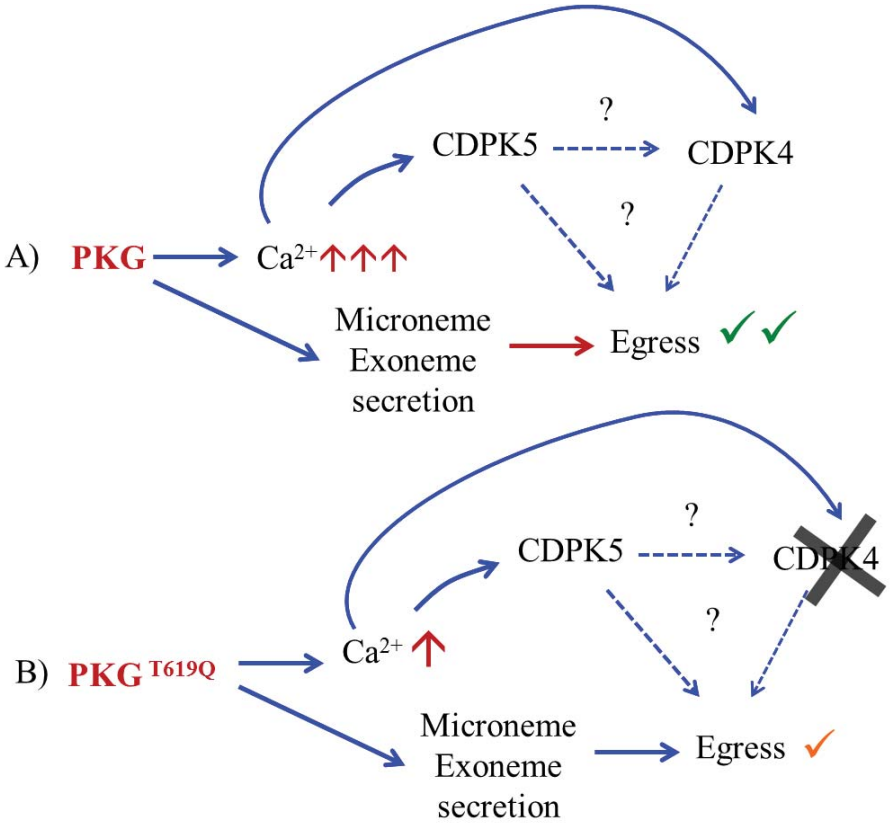

Fig. 5.7| A role for CDPK4 in merozoites egress – a possible model.
(A) Activation of PKG leads to the increase of intracellular calcium that in turn activates CDPK5 and CDPK4. In addition, PKG is also responsible for the discharge of proteases and microneme / exoneme secretion which lead to merozoites egress in a CDPK5-dependent fashion, potentially in cooperation with CDPK4. (B) As the mutated allele of PKG is less efficient at promoting the release of intracellular calcium, the absence of CDPK4 greatly impairs merozoites egress.

The use of hypomorphic alleles enables genetic studies that would not otherwise be possible. The fact that this severe phenotype is not revealed in mutants that only lack the *cdpk4* gene could also mean that a fully functional PKG, but not a hypomorphic allele, is able to divert this signal to an equivalent effector, such as another CDPK.

Follow-up on this matter would involve the inspection of the number of merozoites per schizont to exclude the unlikely possibility of this phenotype being caused by a reduced number of cells per cycle. If this hypothesis is excluded, a transcriptome analysis of *cdpk4* KO and the double mutant, as well as comparative invasion assays, would be crucial to confirm that the decreased fitness is a result of a less efficient egress phenotype. The transcriptome analysis would help clarify whether this phenotype is caused by gene down-regulation of a key factor. It would also be interesting to know whether over-expression of CDPK5 decreases the severity of this phenotype or even if disruption of CDPK5 is possible if CDPK4 is over-expressed.

In addition, as *cdpk4* has a similar role in both *P. berghei* and *P. falciparum*, i.e. it can be deleted in asexual blood stages but blocks microgamete exflagellation [138,143] and a Pb*cdpk4* mutant can be complemented with the Pf*cdpk4* gene [188], it would be interesting to check if the same applies to the interaction with *pkg*. Generation of transgenic parasites is a much longer process in *P. falciparum* than in *P. berghei*, but alternative tools would allow this hypothesis to be tested almost immediately, namely the existence of an equivalent *pkg* point mutation strain (pkg^{T618Q}) [192] and *cdpk4* inhibitors [188].